

## Annealing Effect of Cermet Membranes on Hydrogen Permeability

Sun-Ju Song,<sup>\*1</sup> Eric D. Wachsman,<sup>2</sup> Tae H. Lee,<sup>1</sup> Ling Chen,<sup>1</sup> Stephen E. Dorris,<sup>1</sup> and U. (Balu) Balachandran<sup>1</sup>

<sup>1</sup>Energy Systems Division, Argonne National Laboratory, Argonne, IL 60439, U.S.A.

<sup>2</sup>Department of Materials Science and Engineering, University of Florida, Gainesville, FL 32611, U.S.A.

(Received June 16, 2006; CL-060690; E-mail: song@anl.gov)

Ni–SrCe<sub>0.8</sub>Yb<sub>0.2</sub>O<sub>3–δ</sub> cermet membranes are being developed to separate hydrogen from hydrogen-containing gas mixtures at high temperature. The hydrogen flux of an annealed membrane showed higher flux than that of an as-sintered membrane. The major contribution to overall flux was from ambipolar diffusion through the metal-to-oxide grain boundary. The higher hydrogen permeation flux of an annealed membrane may be understood by its larger metal grains and lower tortuosity, leading to a less-effective length for proton diffusion.

Several technologies are under development for hydrogen production.<sup>1–3</sup> Of these, hydrogen separation membranes<sup>4–6</sup> have received much attention because they function in non-galvanic mode and thus not require electrodes or an external power supply. Separation is purely by ion transport, not a physical process, and yield nearly 100% pure hydrogen with ceramic membranes. Even though the hydrogen permeability may be enhanced by doping with multivalent cations and optimizing the membrane microstructure,<sup>7–9</sup> the reported hydrogen permeability of ceramic membranes is still below that needed for practical use.

Recently, it was reported that cermet membranes exhibit high hydrogen permeation flux with better mechanical strength than ceramics.<sup>10</sup> In cermet membranes, the metal phase is intentionally added to boost the ambipolar conductivity of the membrane by increasing its electronic conductivity and to enhance the catalytic effect on surface exchange reactions. However, the main hydrogen diffusion path through cermet membranes has not been identified yet, and research is necessary on the effect of microstructure on hydrogen permeability.

This work investigated the effect of annealing on the hydrogen permeability of cermet membranes. Under the condition that the oxide property was ensured by similar grain size, the hydrogen permeation flux in the annealed membrane was increased by decreasing the length of the metal-to-oxide grain boundary layer (less tortuosity) with enrichment of effectively positive-charged protons, developed by the negative potential at the metal-to-oxide grain boundary, reference to the bulk oxide.

Polycrystalline SrCe<sub>0.8</sub>Yb<sub>0.2</sub>O<sub>3–δ</sub> powders were prepared by the conventional solid-state reaction method. Oxide powders of SrCO<sub>3</sub> (99.9% Alfa Aesar) and CeO<sub>2</sub> (99.9% Alfa Aesar) were mixed with Yb<sub>2</sub>O<sub>3</sub> (99.99% Alfa Aesar) in a ball mill with stabilized zirconia media in isopropyl alcohol and calcined at 1573 K for 10 h in air. The calcined oxides were then crushed and ground in a ball mill for 24 h. X-ray diffraction spectra confirmed a single phase with an orthorhombic perovskite structure. Nickel cermet membranes were prepared by mixing Ni (Alfa Aesar, 40 vol %) and polycrystalline SrCe<sub>0.8</sub>Yb<sub>0.2</sub>O<sub>3–δ</sub> powders (60 vol %) for 24 h in a ball mill. Then, the mixed powders were pressed into pellets and sintered at 1673 K for 10 h in a nitrogen gas with 200 ppm H<sub>2</sub>. For the coarsening of

metal grain, one pellet membrane was annealed at 1273 K for 4 h in the gas mixture before sintering.

Hydrogen permeation was measured on dense disks (over 96% theoretical density, 0.32-mm thick, 12-mm diameter). The sweep side flow was a constant 100 sccm of 100 ppm H<sub>2</sub>/balance N<sub>2</sub>; the feed gas flow was 100 sccm of 4% H<sub>2</sub>/balance He. For wet gas flow, the feed gas mixture was bubbled through a water bath (EX-35D1 heating bath, Fisher Scientific) at 298 K. The hydrogen content of the permeate stream was measured with a gas chromatograph (HP 6890).

The annealed and as-sintered membranes were conductive, indicating that a three-dimensional network of Ni phase had formed, and hydrogen flux might be limited by proton flux. Because atomic hydrogen diffusion through the Ni phase is also detectable under some conditions, the total hydrogen flux through cermet membranes can be expressed as the sum of ambipolar and atomic diffusion:

$$J_{\text{H}_2} = - \left( \frac{xRT}{4LF^2} \int_{P_{\text{H}_2}^{\text{sweep}}}^{P_{\text{H}_2}^{\text{feed}}} \frac{\sigma_{\text{OH}_2} \sigma_{\text{e}}'}{\sigma_{\text{OH}_2} + \sigma_{\text{e}}'} d \ln P_{\text{H}_2} + (1-x) \frac{\Phi}{L} \Delta P_{\text{H}_2}^{1/2} \right), \quad (1)$$

where  $L$  is the thickness of the membrane,  $F$  is the Faraday constant,  $P_{\text{H}_2}$  is the chemical potential gradient across a membrane,  $x$  is volume fraction of oxide,  $\Phi$  is the hydrogen permeability of Ni, and  $\sigma_i$  is the partial conductivity of the charged species. The solubility of atomic hydrogen in the metallic phase was determined by Sievert's law by assuming a dilute solution.

The temperature dependences of the hydrogen flux of 0.32-mm-thick cermet membranes are shown in Figure 1. For both membranes, the hydrogen fluxes increase with temperature, and the annealed membrane shows higher flux than the as-sintered membrane. The back-scattering scanning electron

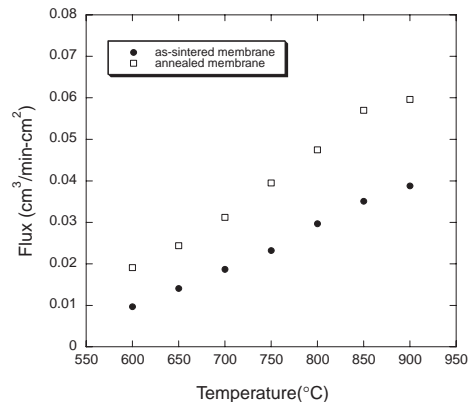


**Figure 1.** Hydrogen permeation flux of annealed and as-sintered membranes in wet 4% H<sub>2</sub>/balance He.

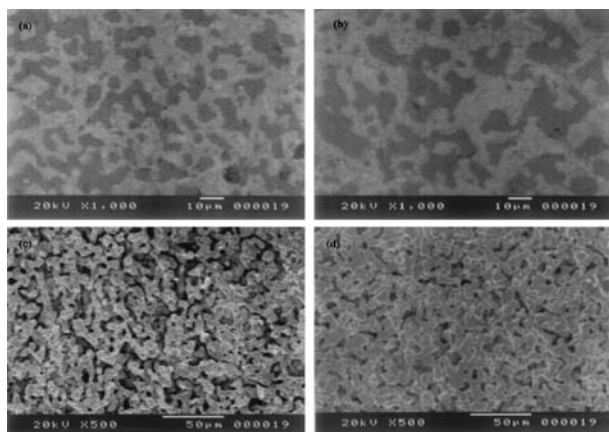


**Figure 2.** SEM micrographs of (a) as-sintered and (b) annealed Ni-Yb-doped SrCeO<sub>3</sub>, and (c) as-sintered and (d) annealed membrane after being etched with HNO<sub>3</sub>.

micrographs (Figure 2) of the cermet membranes show the metal grain sizes (black color in images) in their microstructures. The grain size of the oxide phase was expected to be similar because the two membranes were sintered at the same temperature with the same starting oxide powders.

Previous work showed that the bulk transport of protons makes a major contribution to the total conductivity at higher temperature due to the lower bulk resistance.<sup>9</sup> So a larger grain size of the oxide phase should improve proton transport. The grain size of the oxide phase for both membranes was close, as shown in Figure 2, so that the difference in hydrogen permeation flux may not be attributed to differences in either oxide grain size or oxide-to-oxide grain boundaries. It is known that the grain size of the metal phase does not influence the hydrogen permeability of metal down to the submicron.<sup>11,12</sup> Therefore, the difference in hydrogen permeation flux may be attributed to the interfacial properties between the metal and oxide phase.

The hydrogen flux through nickel phase was calculated from the permeability data<sup>13</sup> as a function of temperature under the applied hydrogen potential gradients. By subtracting the metal and oxide phase contribution to total flux, the contribution through interfacial diffusion was calculated to be dominant in the temperature range investigated. The metal-to-oxide interfacial diffusion can be a distinct feature compared to single-phase membranes. Therefore, the difference in the hydrogen flux between the annealed and as-sintered membrane may be explained by the metal-to-oxide interfacial diffusion. Because the major contribution to overall flux was from ambipolar diffusion through the metal-to-oxide grain boundary, the higher hydrogen flux of the annealed membrane may be attributed to its greater metal grain size and lesser tortuosity, leading to a less-effective length for proton diffusion. The interfacial ambipolar diffusion through the metal-to-oxide interface can further be understood by the space charge layer,<sup>14–16</sup> because cermet membrane consists of two phases having different electrochemical potentials. Because the electron chemical potential of the metal phase is sufficiently higher than that of the oxide phase, the negative potential at the grain boundary, reference to the bulk ( $\phi_0 < \phi_\infty = 0$ ), may be developed, the curvature of which is related to the charge density and thus the defect concentration according

to Poisson's equation. Therefore, the concentration of the effectively positive-charged protons may increase in the grain boundary layer (space charge layer) between the metal and oxide phase. It is assumed that the grain is large with respect to the space-charge layer width and also large enough that the proton enrichment to the grain boundary layer does not appreciably deplete the bulk proton concentration. It should also be mentioned that the interfacial area becomes small by annealing (Figure 2d), leading to that the volume fraction of space charge layer may decrease. However, the overall permeation flux was limited by bulk diffusion in the thickness investigated and the space-charge volume change may not be critical factor to overall hydrogen flux.

To summarize, under the condition that the oxide property was ensured by similar grain size, the hydrogen permeation flux with an annealed membrane increased because of the decrease in the length of metal-to-oxide grain boundary layer with enrichment of effectively positive charged protons, developed due to the negative potential at grain boundary, reference to the bulk oxide ( $\phi_0 < \phi_\infty = 0$ ). Therefore, the metal-to-oxide grain boundary layer may provide a fast ambipolar diffusion path for cermet membranes.

This work was supported by the U.S. Department of Energy, Office of Fossil Energy, National Energy Technologies Program, under Contract W-31-109-Eng-38.

## References

- 1 A. F. Sammells, M. Schwartz, R. A. Mackay, T. F. Barton, D. R. Peterson, *Catal. Today* **2000**, 56, 325.
- 2 J. C. De Deken, E. F. Devos, G. F. Froment, *Chemical Reaction Engineering ACS Symposium Series*, Washington DC, U.S.A., p. 196.
- 3 H. Iwahara, *Solid State Ionics* **1995**, 77, 289.
- 4 H. Iwahara, T. Esaka, H. Uchida, N. Maeda, *Solid State Ionics* **1981**, 3–4, 359.
- 5 S. Hamakawa, L. Li, A. Li, Iglesia, *Solid State Ionics* **2002**, 148, 71.
- 6 X. Qi, Y. S. Lin, *Solid State Ionics* **2000**, 130, 149.
- 7 S.-J. Song, E. D. Wachsman, J. Rode, H.-S. Yoon, K.-H. Lee, G. Zhang, S. E. Dorris, U. Balachandran, *J. Mater. Sci.* **2005**, 40, 4061.
- 8 S.-J. Song, E. D. Wachsman, J. Rhodes, S. E. Dorris, U. Balachandran, *Solid State Ionics* **2004**, 167, 99.
- 9 S.-J. Song, E. D. Wachsman, J. Rhodes, S. E. Dorris, U. Balachandran, *Solid State Ionics* **2003**, 164, 107.
- 10 S.-J. Song, T. H. Lee, E. D. Wachsman, L. Chen, S. E. Dorris, U. Balachandran, *J. Electrochem. Soc.* **2005**, 152, J125.
- 11 S. Heinze, B. Vuillemin, J.-C. Colson, P. Giroux, D. Leterq, *Solid State Ionics* **1999**, 122, 51.
- 12 R. Kirchheim, *Acta Metall.* **1981**, 29, 835.
- 13 S. A. Steward, *Review of Hydrogen Isotope Permeability Through Materials*, Lawrence Livermore National Laboratory, University of California, Livermore, California, ICR:53441, DE84 007362.
- 14 J. Maier, *Ber. Bunsen-Ges. Phys. Chem.* **1986**, 90, 26.
- 15 J. Maier, *J. Electrochem. Soc.* **1987**, 134, 1524.
- 16 X. Guo, W. Sigle, J. Maier, *J. Am. Ceram. Soc.* **2003**, 86, 77.